The Blackwood Creek Reach 6 Restoration Project's Influence on Reach Scale Sediment Scour and Storage Characteristics

by

David Raymond Immeker

A plan B paper submitted in partial fulfillment
of the requirements for the degree

of

MASTER OF SCIENCE

in

Watershed Science

Approved:

John C. Schmidt Major Professor	Tom Lachmar Committee Member

Chris Luecke
Committee Member

UTAH STATE UNIVERSITY

Logan, Utah

2012

ABSTRACT

The Blackwood Creek Reach 6 Restoration Project's Influence on
Reach Scale Sediment Scour and Storage Characteristics

By

David Immeker
Utah State University, 2012

Major Professor: Dr. John C. Schmidt
Department: Watershed Sciences

Stream restoration activities in Reach 6 of Blackwood Creek involved constructing a new stream channel in a reach that had been eroding and adjusting to historic land uses since the 1960s. In 2010, the spring after restoration work was completed, the project had a 2.3-year recurrence peak flow of 12.3 m^3/s. This post-project assessment looks at the impacts of restoration work in Reach 6 in the short time since the project was completed. Project objectives for restoration work were to: increase the extent of floodplain inundation for seasonal flooding, reduce the rate of bank erosion, and to encourage sediment deposition, particularly fine sediment, on the floodplain.

Using HEC-RAS, a one dimensional hydrologic model, I predict that the extent of flooding over a wide range of recurrences will increase as a result of restoration work, with the largest proportional increase for small magnitude, high recurrence floods. To assess the impact restoration activities will have on stream channel erosion, the average predicted shear stress was compared between pre-restoration and post-restoration conditions. This work indicates that there will be a decrease in average shear stress for all floods, with a 39% decrease for the 1.5-year recurrence flow and a 48% decrease for a 20-year recurrence flow. In 2010, areas of deposition

and scour were mapped in Reach 6 to assess whether the project reach was accumulating sediment on the floodplain. I found that 1,129 m^3 of sediment had been deposited and 142 m^3 of sediment has been scoured. Of the 1,541 Mg of sediment deposited within Reach 6, 40% was gravel and coarser sizes, 50% was sand, 7% was silt, and 2% was clay.

CONTENTS

LIST OF FIGURES vi
Chapter 1-Introduction 1
1.1 Blackwood Creek Watershed 3
1.2 Recent Land Use History 5
1.3 Aerial Photo Record of Reach 6 9
1.4 Previous Restoration Work in Blackwood Canyon 15
1.5 Previous Post-Project Assessment Work 16
1.6 Research Objectives 20
Chapter 2-Methods and Data Collection 21
2.1 Hydraulic Modeling 21
2.2 Building the HEC-RAS/HEC Geo-RAS Model 24
2.3 Sediment Deposition/Scour Mapping and Sampling 29
Chapter 3-Results and Discussion 37
3.1 Hydraulic Modeling 37
3.2 Sediment Deposition/Scour Mapping and Sampling 39
3.3 Discussion 43
Chapter 4-Conclusion 46
References Cited 48
Appendix 51
Pre-Restoration Area Inundated by Water 51
Post-Restoration Area Inundated by Water 56
Terrain Models Used for HEC-RAS Modeling 61
Sediment Deposition/Scour Maps 62
1969 Gravel Mine and Reach 6 Overview 64
Gravel Mine Location Maps from 1939 and 1969 65
Sediment Deposition/Scour Mapping Summary Data 66
Sediment Sampling Locations 70
HEC-RAS Model Run Outputs 71
Pre-restoration HEC-RAS model run summary for a 3-year recurrence flow of 16 m^3/s 71
Post-restoration HEC-RAS model run summary for 3-year recurrence flow of 16 m^3/s. 77
HEC-RAS Modeled Shear Stress Summary 92

LIST OF TABLES

Table 1. This table summarizes some of the significant historic periods in Blackwood Canyon. 6
Table 2. This table shows the decrease in sinuosity observed in Reach 6 as identified in the available aerial photos 9
Table 3. Table 3 shows the discharge measurements taken in July 2011 and the Manning's n that was calculated for that discharge. 26
Table 4. This table compares the water surface elevation with the modeled water surface elevation once the HEC-RAS model was calibrated to a discharge of 12.3 m^3/s. Distance upstream is the distance up the channel from the downstream Reach 6 project boundary. The elevation difference is the surveyed elevation minus the modeled elevation. 28
Table 5. This table shows instantaneous peak flows at Reach 6 used to model the area inundated by water and shear stress. Flows were acquired from the USGS gage #10336660, Blackwood Creek Near Tahoe City California located at the mouth of Blackwood Canyon (USGS, 2011) and scaled down to the watershed for Reach 6. 29
Table 6. This table compares the dry bulk sample mass to the mass of the largest single particle in the sample for bulk samples. 35
Table 7. This table compares the modeled flooded area between the 2007 pre-restoration conditions and the 2010 post-restoration conditions for a range of flows. 37
Table 8. This table shows the average cross-sectional shear stress that was modeled in HEC-RAS for pre-restoration conditions and post-restoration conditions for a range of flows. 38
Table 9. This table shows the area and volume of areas of deposition, scour and mixed areas (areas showing a mixture of deposition and scour) that were mapped in the summer of 2010 in Reach 6. 40
Table 10. This table shows weight in megagrams of the gravel and coarser, sand, silt and clay in the areas of deposit and scour. Also shown is whether there was more deposition or scour for each size class and what the difference was between the two values. 40
Table 11. This table shows the surface grain size class, area, depth, volume and polygon number of deposition polygons that were mapped in the summer of 2010. 68
Table 12. This table shows the area, depth, volume and polygon number of scour polygons that were mapped in the summer of 2010. 69
Table 13. Pre-restoration HEC-RAS model run summary for a 3-year recurrence flow of 16 m^3/s. 77
Table 14. Post-restoration HEC-RAS model run summary for 3-year recurrence flow of 16 m^3/s. 91
Table 15. This table shows the standard deviation of the cross section shear stresses calculated in HEC-RAS for each model run for both before restoration and after restoration conditions. 92

LIST OF FIGURES

Figure 1. An overview map showing the location of Reach 6 in the Blackwood Creek watershed on the west shore of Lake Tahoe, near the California/Nevada state line 4
Figure 2. The 1939 aerial photo of Blackwood Creek Reach 6. The blue line is the alignment of the channel and the red lines show the extent of the Reach 6 restoration project area. Sinuosity in this photo was 1.80 and by 2007, sinuosity decreased to 1.23 as the channel straightened. Note the dense vegetation found on both sides of the channel. Stream flow is to the east. 10
Figure 3. The 1969 aerial photo of Blackwood Creek Reach 6. The blue line is the alignment of the channel and the red lines show the extent of the Reach 6 restoration project area. Note logging on the floodplain in the western portion of the photo. Stream flow is to the east. 11
Figure 4. The 1986 aerial photo of Blackwood Creek Reach 6. The blue line is the alignment of the channel and the red lines show the extent of the Reach 6 restoration project area. Note how unvegetated washes have formed near the channel. Stream flow is to the east. 11
Figure 5. The 1995 aerial photo of Blackwood Creek Reach 6. The blue line is the alignment of the channel and the red lines show the extent of the Reach 6 restoration project area. Stream flow is to the east. 12
Figure 6. The 2001 aerial photo of Blackwood Creek Reach 6. The blue line is the alignment of the channel and the red lines show the extent of the Reach 6 restoration project area. Between this photo and the 1995 photo was the flood of record at78 m^3/s. Stream flow is to the east. 13
Figure 7. The 2007 aerial photo of Blackwood Creek Reach 6. The blue line is the alignment of the channel and the red lines show the extent of the Reach 6 restoration project area. By 2007, sinuosity had decreased to1.23, compared to 1.80 that was seen in 1939. Stream flow is to the east. 13
Figure 8. Log Pearson type III flood frequency analysis for the downstream end of Blackwood Creek Reach 6. Instantaneous peak flows were taken from the USGS gage #10336660, Blackwood Creek Near Tahoe City California located at the mouth of Blackwood Canyon (USGS, 2011) and scaled down to the watershed for Reach 6. 38
Figure 9. This graph shows the average cross section shear stress of the channel and floodplain that was modeled in HEC-RAS for pre-restoration conditions and post-restoration conditions for a range of flows. 39
Figure 10. Map showing the modeled area inundated with water by the HEC-RAS/HEC Geo-RAS modeled 2.3-year, 12.3 m^3/s flow and the areas of deposition, scour and areas that had both deposition and scour that were mapped in the summer of 2010. 41
Figure 11. The weight in megagrams of the deposition and scour for each size class used in this study as well as the total weight of deposition and scour. 42
Figure 12. August 17, 2007 aerial photo of Blackwood Creek Reach 6 (before restoration work) with the area inundated by water for a HEC-RAS/HEC Geo-RAS modeled 2.3-year, 12.3 m^3/s flow, the peak flow that occurred in the spring of 2010. The area inundated by water is 17,150 m^2. 51
Figure 13. August 17, 2007 aerial photo of Blackwood Creek Reach 6 (before restoration work) with the area inundated by water for a HEC-RAS/HEC Geo-RAS modeled 1.5-year, 7.4 m^3/s flow. The area inundated by water is 14,836 m^2. 51

Figure 14. August 17, 2007 aerial photo of Blackwood Creek Reach 6 (before restoration work) with the area inundated by water for a HEC-RAS/HEC Geo-RAS modeled 2-year, 10.7 m^3/s flow. The area inundated by water is 19,951 m^2. 52
Figure 15. August 17, 2007 aerial photo of Blackwood Creek Reach 6 (before restoration work) with the area inundated by water for a HEC-RAS/HEC Geo-RAS modeled 3-year, 16 m^3/s flow. The area inundated by water is 19,951 m^2. 52
Figure 16. August 17, 2007 aerial photo of Blackwood Creek Reach 6 (before restoration work) with the area inundated by water for a HEC-RAS/HEC Geo-RAS modeled 4-year, 20 m^3/s flow. The area inundated by water is 22,952 m^2. 53
Figure 17. August 17, 2007 aerial photo of Blackwood Creek Reach 6 (before restoration work) with the area inundated by water for a HEC-RAS/HEC Geo-RAS modeled 5-year, 23 m^3/s flow. The area inundated by water is 29,731 m^2. 53
Figure 18. August 17, 2007 aerial photo of Blackwood Creek Reach 6 (before restoration work) with the area inundated by water for a HEC-RAS/HEC Geo-RAS modeled 10-year, 37 m^3/s flow. The area inundated by water is 39,237 m^2. 54
Figure 19. August 17, 2007 aerial photo of Blackwood Creek Reach 6 (before restoration work) with the area inundated by water for a HEC-RAS/HEC Geo-RAS modeled 15-year, 47 m^3/s flow. The area inundated by water is 41,377 m^2. 54
Figure 20. August 17, 2007 aerial photo of Blackwood Creek Reach 6 (before restoration work) with the area inundated by water for a HEC-RAS/HEC Geo-RAS modeled 20-year, 55 m^3/s flow. The area inundated by water is 43,664 m^2. 55
Figure 21. November 3, 2010 aerial photo of Blackwood Creek Reach 6 (after restoration work) with the area inundated by water for a HEC-RAS/HEC Geo-RAS modeled 2.3-year, 12.3 m^3/s flow, the peak flow that occurred in the spring of 2010. The area inundated by water is 32,276 m^2. 56
Figure 22. November 3, 2010 aerial photo of Blackwood Creek Reach 6 (after restoration work) with the area inundated by water for a HEC-RAS/HEC Geo-RAS modeled 1.5-year, 7.4 m^3/s flow. The area inundated by water is 29,394 m^2. 56
Figure 23. November 3, 2010 aerial photo of Blackwood Creek Reach 6 (after restoration work) with the area inundated by water for a HEC-RAS/HEC Geo-RAS modeled 2-year, 10.7 m^3/s flow. The area inundated by water is 34,188 m^2. 57
Figure 24. November 3, 2010 aerial photo of Blackwood Creek Reach 6 (after restoration work) with the area inundated by water for a HEC-RAS/HEC Geo-RAS modeled 3-year, 16 m^3/s flow. The area inundated by water is 34,188 m^2. 57
Figure 25. November 3, 2010 aerial photo of Blackwood Creek Reach 6 (after restoration work) with the area inundated by water for a HEC-RAS/HEC Geo-RAS modeled 4-year, 20 m^3/s flow. The area inundated by water is 35,566 m^2. 58
Figure 26. November 3, 2010 aerial photo of Blackwood Creek Reach 6 (after restoration work) with the area inundated by water for a HEC-RAS/HEC Geo-RAS modeled 5-year, 23 m^3/s flow. The area inundated by water is 41,374 m^2. 58
Figure 27. November 3, 2010 aerial photo of Blackwood Creek Reach 6 (after restoration work) with the area inundated by water for a HEC-RAS/HEC Geo-RAS modeled 10-year, 37 m^3/s flow. The area inundated by water is 50,235 m^2. 59

Figure 28. November 3, 2010 aerial photo of Blackwood Creek Reach 6 (after restoration work) with the area inundated by water for a HEC-RAS/HEC Geo-RAS modeled 15-year, 47 m^3/s flow. The area inundated by water is 52,004 m^2. 59
Figure 29. November 3, 2010 aerial photo of Blackwood Creek Reach 6 (after restoration work) with the area inundated by water for a HEC-RAS/HEC Geo-RAS modeled 20-year, 55 m^3/s flow. The area inundated by water is 54,379 m^2. 60
Figure 30. Pre-restoration (2007) triangular irregular network (TIN) generated from one foot contour lines. This TIN was used in HEC-RAS/HEC Geo-RAS modeling. 61
Figure 31. Post-restoration (2010) triangular irregular network (TIN) generated from one foot contour lines. This TIN was used in HEC-RAS/HEC Geo-RAS modeling. 61
Figure 32. West half of the map showing the unique number assigned to each polygon. 62
Figure 33. East half of the map showing the unique number assigned to each polygon. 63
Figure 34. Map showing Blackwood Creek from the gravel mine, downstream to Reach 6. Blackwood Creek is in the diversion channel (in red) in this 1969 aerial photo. 64
Figure 35. Gravel mine location in 1939 before gravel mining started. 65
Figure 36. Gravel mine in 1969 with Blackwood Creek in the diversion channel around the mine. This aerial photo shows the same location as the 1939 photo above. 65
Figure 37. Map showing the location where sediment samples were taken in the summer of 2010. 70

Chapter 1-Introduction

Stream restoration post-project appraisals have been defined as "systematic assessments of built restoration projects, which provide feedback on performance of restoration approaches to improve future restoration efforts" (Kondolf et al., 2011). Monitoring the status and performance of stream restoration projects with a post-project appraisal allows us to learn from our mistakes or successes and make better informed decisions in the future. Downs and Kondolf (2002) propose that performing post-project appraisals can "evaluate river restoration schemes in relation to their compliance with design, their short-term performance attainment, and their longer-term geomorphological compatibility with the catchment hydrology and sediment transport processes." Wohl et al. (2005) propose that stream restoration projects can be viewed as experiments and that only by systematically monitoring each project can we learn from each project's successes and failures.

Most restoration projects are not monitored. As of 2005, over $ 1billion were being spent annually on stream restoration projects in the United States, and yet, once completed, few projects receive any sort of post-project appraisal (Bernhardt et al. 2005). In a survey of California restoration projects, the National River Restoration Science Synthesis group found that only 11% of restoration projects in their survey were monitored (National River Restoration Science Synthesis, 2006). In order to determine whether a restoration project was successful in achieving its objectives or if it was performing as designed, some level of monitoring is required. In addition, it is useful for project objectives to be stated in the planning phase of a restoration project. Projects with stated, quantifiable objectives have a standard to which the project can be compared to determine if the project was successful (Kondolf, 1995).

In the summer of 2008 and 2009, the US Forest Service implemented a stream restoration project in Blackwood Canyon on the west shore of Lake Tahoe, California. This watershed was selected for restoration, because it has been identified as the second largest sediment producing watershed in the Lake Tahoe basin (Simon et. al, 2004). In 2003, Swanson (2003) classified the reaches of lower Blackwood Creek based upon a geomorphic analysis. Reach 6 was the number assigned to the stream reach that is the subject of this post-project appraisal. This restoration project entailed reconstructing the stream channel and floodplain, because this segment had experienced high erosion rates since the 1960s (Swanson, 2003; Kiesse, 2011).

Restoration work entailed constructing a series of large rock-log roughness structures that were designed and positioned to redirect flows into a more sinuous, less entrenched, channel. A more sinuous flow path at higher base level was constructed between the roughness structures. The design of the project allows the position of the channel to shift laterally. Excessive movement of the channel in response to sediment and woody debris inputs expected during rain-on-snow flood conditions is limited by roughness structures. Channel and floodplain aggradation is expected over the long term, given that watershed conditions upstream are thought to still be recovering from land use impacts. Roughness structures are multi-purposed. Their positioning discourages high energy flows from directly eroding high terrace cut banks composed primarily of sand and mud, and creates lee side low velocity regions that encourage sediment deposition (USFS, 2011, Craig Oehrli, USFS Hydrologist, personal communication). In spring 2010, following the completion of the project, Reach 6 was inundated by a 2.3-year recurrence flood of 12.3 m^3/s. After flows receded, areas of deposition and erosion were observed on the floodplain.

The goal of this analysis is to evaluate whether the restoration project in Reach 6 of Blackwood Creek was successful in meeting its objectives and whether the project performed

consistent with the project design. To determine this, project objectives were taken from the project environmental assessment report (USDA, 2008). From the objectives, monitoring questions were developed to determine if the project has, in the short term, been successful in achieving these objectives. In the year after the restoration project was completed, the project area did begin to respond by forming many new areas of deposition and scour on the floodplain and along the channel.

1.1 Blackwood Creek Watershed

The Blackwood Creek watershed drains into the western part of Lake Tahoe in the Sierra Nevada Mountains of California. The western part of the watershed is the primary drainage divide of the Sierra Nevada, and Blackwood Creek drains to the east (Figure 1). The watershed area is 29 km^2 and ranges in elevation from 2,706 m at Twin Peaks to 1,897 m at Lake Tahoe.

The Blackwood Creek watershed is predominantly underlain by volcanic rocks with a predominance of andesitic and basaltic rocks. Overlying the volcanic parent material are numerous fluvial and glacial deposits. The Blackwood Creek valley has a U-shape, typical of most of the valleys in the region that were extensively glaciated. There are many extensive and large landslides in the valley (Swanson, 2003).

Soils in the watershed are predominantly derived from volcanic parent material. Steeper slopes higher in the watershed tend to have less well developed thin soils with many locations of exposed bedrock. Lower in the valley, soils are more developed and deeper. Many of the lower elevation areas are composed of soils that have formed on glacial outwash and alluvial fans.

Flood flows are typically caused by one of two processes. The spring melt each year typically creates the annual instantaneous peak flow. The highest spring snowmelt peak flow for

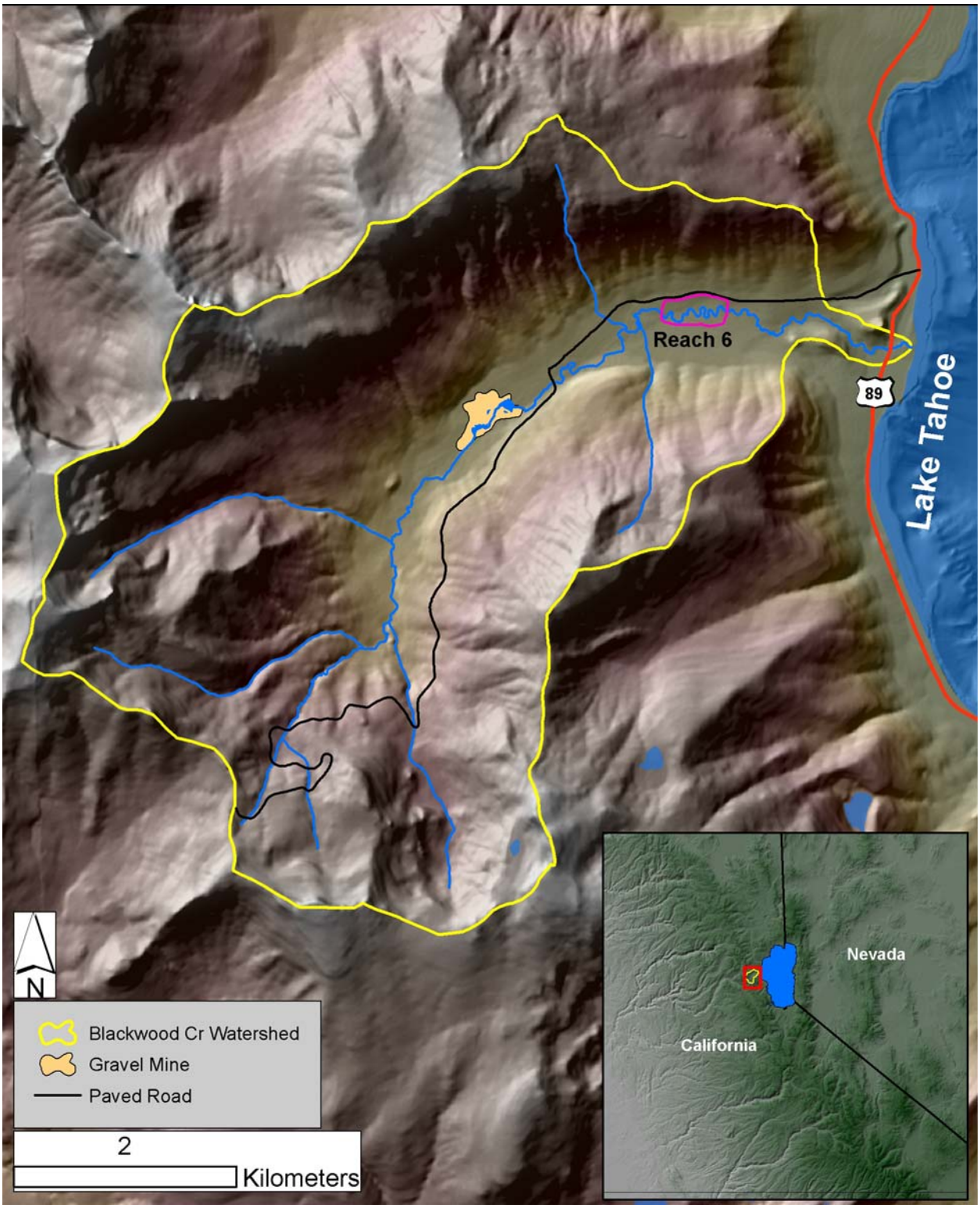

Figure 1. An overview map showing the location of Reach 6 in the Blackwood Creek watershed on the west shore of Lake Tahoe, near the California/Nevada state line

the period of record for the USGS gage at the mouth of Blackwood Canyon was 27 m^3/s on May 16, 1996. Rarer but larger peak flows occur in some years and are usually caused by rain-on-snow events. The highest instantaneous peak flow recorded for Blackwood Creek was 83 m^3/s on January 1, 1997, during a rain-on-snow event.

1.2 Recent Land Use History

The Blackwood Creek watershed was heavily used from the late 1800s to approximately 1970 for livestock grazing, logging, and gravel mining (Table 1). The earliest documented sheep grazing in Blackwood Canyon dates back to 1865, and in 1889, clear cut logging began in the lower 2.5 km of the watershed. Through the 1960s, grazing ceased but logging increased in intensity. In 1960, a gravel mine began operating along Blackwood Creek and the adjacent floodplain, and Blackwood Creek was diverted around the mine in a diversion channel (Tetra Tech, 1999).

By the late 1800s, most suitable land in Blackwood Canyon was grazed by sheep. A report written in 1905 commented that Blackwood Canyon was being heavily grazed. In 1944, a US Forest Service report on Blackwood Canyon expressed concern over the deterioration of meadows and increased erosion from overgrazing. In 1959, a US Forest Service range report recommended closing Blackwood Canyon to grazing due to deterioration of meadows and valley bottoms from overgrazing. By 1963, nearly all grazing in Blackwood Canyon had stopped (Tetra Tech, 1999).

Extensive logging in Blackwood Canyon began in the 1950s when most of the watershed was still privately owned. By 1956, enough timber was being generated from Blackwood Canyon that a sawmill was built along Blackwood Creek. To provide timber to the mill, an

Year	Event
1865	Earliest recorded sheep grazing in Blackwood Creek watershed
1889-1905	Clear-cut logging along Blackwood Creek in lowest 2.4 km of the watershed
1953-1962	Extensive logging and logging road construction throughout Blackwood Canyon
1960	Gravel mining starts 1.5 km upstream of Reach 6 and Blackwood Creek diverted around gravel mining operation in diversion channel
1962	Grazing ends in Blackwood watershed
1968	California Department of Fish and Game removes woody debris and beaver dams from Blackwood Creek to remove fish passage barriers
1968	Gravel mine ceases operation
1969	Diversion channel around gravel mine is cut off and Blackwood Creek is diverted back into its original alignment, through the gravel pit
1971	Large scale logging ceases in Blackwood watershed
1971	Woody debris removed from channel downstream from gravel mine location, through Reach 6 by Lake Tahoe Area Council for fish passage

Table 1. This table summarizes some of the significant historic periods in Blackwood Canyon.

extensive system of roads was constructed throughout the canyon that can be clearly seen in the 1969 aerial photo of the Blackwood Creek watershed. By 1969, most of the lower elevation, easily accessible portions of the watershed had been logged, including the floodplain. By 1970, the US Forest Service had acquired nearly the entire Blackwood Creek watershed, and large scale logging operations stopped (Tetra Tech, 1999). Logging on the floodplain removed many trees that would have eventually died, fallen, and become important roughness elements that would have reduced velocities during flood flows over the floodplain and along the stream. In addition to commercial logging, in the late 1960s, woody debris was removed from Blackwood Creek, downstream from the gravel mine location, in an effort to remove fish passage barriers.

Several reports have proposed that logging and overgrazing have impacted the hydrologic response time and erosion rate in the watershed. Swanson (2003) hypothesized that the extensive network of roads and skid trails in the watershed contributed to channel and floodplain instability by more effectively routing water to Blackwood Creek. This would have produced a flashier

response to rain and could lead to higher peak flows in Blackwood Creek. In addition, Kiesse (2011) believes that overgrazing and logging would have increased the upland erosion rate and provided additional sediment to the creek. However, he also believes that, while overgrazing and increased erosion due to grazing and logging may have contributed to the channel instability in Blackwood Creek, it was not the primary factor responsible. The primary channel instability trigger is thought to be in-stream gravel mining at the head of the valley.

With development and associated road building in the Lake Tahoe basin in the 1950s and 1960s came the demand for aggregate. A mining operation in Blackwood Canyon began in 1960. The location of the gravel mine, 1.5 km up valley from Reach 6, was along Blackwood Creek where the channel slope decreases and the valley bottom widens substantially. In 2001, Swanson Hydrology and Geomorphology surveyed a long profile of the thalweg of Blackwood Creek where it flows through the former gravel mine pit. They found that the 1,090-m reach upstream of the gravel mine had a slope of 0.0120, while the slope for the 510-m long channel in the gravel mine decreased to 0.0036. On the down valley side of a landslide that is downstream from the gravel mine site, the channel slope once again increases to 0.0106 for 490 m (Swanson, 2003). This reach of low channel slope has been an area of coarse bedload aggradation since the landslide occurred and was therefore a logical location to locate a gravel mining operation (Tetra Tech, 1999). This decrease in channel slope and valley widening was caused naturally by a landslide coming off the north side of Blackwood Canyon and covering the valley bottom, around 300 to 15,000 YBP (Swanson, 2003). The landslide caused a natural discontinuity in sediment transport with substantial bedload deposition up valley from the landslide.

In 1960, Blackwood Creek was diverted into a diversion canal around the gravel mine. The aerial photos of the stream reach through the gravel mine pit before mining show that the

stream had a sinuosity of 1.59. The diversion canal that was built around the gravel pit was much straighter (sinuosity decreased to 1.14) and therefore must have had a greater slope through the reach. The increase in slope increased the stream competence, and the stream therefore was able to transport bedload coming in from upstream that was previously deposited in the low slope reach upstream of the landslide. This means that areas downstream of the landslide began receiving bedload that was previously being deposited on the low slope reach upstream from the landslide (Tetra Tech, 1999; Swanson, 2003; Kiesse, 2011; Gavigan, 2007). Additionally, Kiesse (2011) believes that the diversion canal itself was likely an additional source of coarse material to the downstream reach as the diversion canal widened and incised.

Several watershed assessments written on Blackwood Canyon propose that gravel mining activities, and specifically the re-routing of Blackwood Creek through the diversion canal, had the greatest impact on the destabilization of Blackwood Creek (Tetra Tech, 1999; Tetra Tech, 2001; Swanson, 2003; Gavigan, 2007; Kiesse, 2011). By routing an abundance of bedload through the diversion canal, reaches immediately downstream of the gravel mine pit began receiving more bedload than had been occurring previously. Before, these reaches received a minimal amount of bedload because of the upstream geomorphic controls described earlier. The combined effects of adding bed load and logging near the stream then set channel and floodplain destabilization in motion. Invading bedload would have been deposited onto the inside of meanders during periods of high flow. The building point bars caused erosive power to be applied to the outside of meanders. As bank erosion and point bar formation progressed, the channel slope would have decreased. In addition, the material eroded from the outside of meanders would then add to the excess of sediment in the channel and be transported downstream to Reach 6. This excess of sediment aggraded the channel and may have even

decreased the width to depth ratio temporarily. The combination of an aggrading channel and flood flows passing over a smoother, less erosion-resistant floodplain enhanced destabilization by allowing the creek to cut off meanders, thus shortening and steepening the channel bed. Once the channel had straightened and steepened, Blackwood Creek then had more competence and incised its bed. After incision, flood flows, that previously were able to dissipate over the floodplain, were contained within the channel. The increase in shear stress within the channel caused increased bank erosion in all reaches downstream from the gravel mine and a new lower elevation floodplain began to form (Tetra Tech, 1999; Swanson, 2003; Gavigan, 2007; Kiesse, 2011).

1.3 Aerial Photo Record of Reach 6

Comparing changes between the 1939 and 2007 air photos shows that there was a decrease in sinuosity from 1.80 to 1.23 in 68 years (Table 2). In addition, the floodplain in 1939 appears to be covered in dense vegetation. Accounts of the floodplain in the early 1940s indicate that most of the valley bottom floodplain was composed of a series of meadows intermixed with cottonwood forests (Tetra Tech, 1999). While the species present in the 1939 aerial photo cannot be determined, it is clear that the extensively vegetated floodplain present in 1939 had been replaced by 2007 with open gravel washes that were mostly devoid of vegetation.

Year	Channel Length (m)	Sinuosity
1939	985	1.80
1969	894	1.63
1986	835	1.53
1995	777	1.42
2001	731	1.34
2007	674	1.23

Table 2. This table shows the decrease in sinuosity observed in Reach 6 as identified in the available aerial photos

The 1939 aerial photo (Figure 2) is the earliest aerial photo of Reach 6. In this photo, the floodplain appears to have a uniform cover of vegetation on it. The dense vegetation, in addition to the lower quality photography, makes it difficult to locate the channel accurately in some locations. Comparing the 1939 aerial photos to the 1969 aerial photo (Figure 3) shows that in the intervening 30 years, a large portion of the floodplain directly adjacent to the channel was logged. In 1939, the channel sinuosity was 1.8, and by 1969, sinuosity had decreased slightly to 1.63.

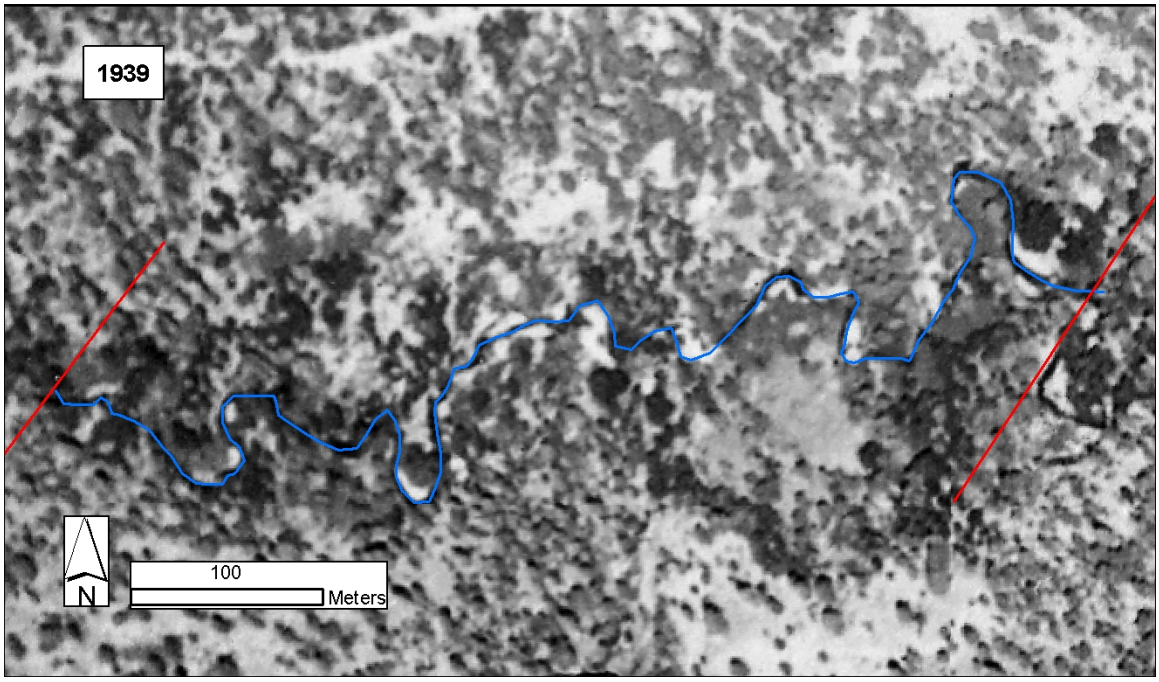

Figure 2. The 1939 aerial photo of Blackwood Creek Reach 6. The blue line is the alignment of the channel and the red lines show the extent of the Reach 6 restoration project area. Sinuosity in this photo was 1.80 and by 2007, sinuosity decreased to 1.23 as the channel straightened. Note the dense vegetation found on both sides of the channel. Stream flow is to the east.

Comparing the 1969 aerial photo to the 1986 photo (Figure 4) shows that that the channel in Reach 6 had begun to change substantially. In the upper half of Reach 6, the channel had cut across several meanders and much of the vegetation that existed on the floodplain adjacent to the channel had been removed and been replaced by un-vegetated gravel washes. In the lower half of reach 6, the channel was still in the same location. During the 17-year period between the 1969

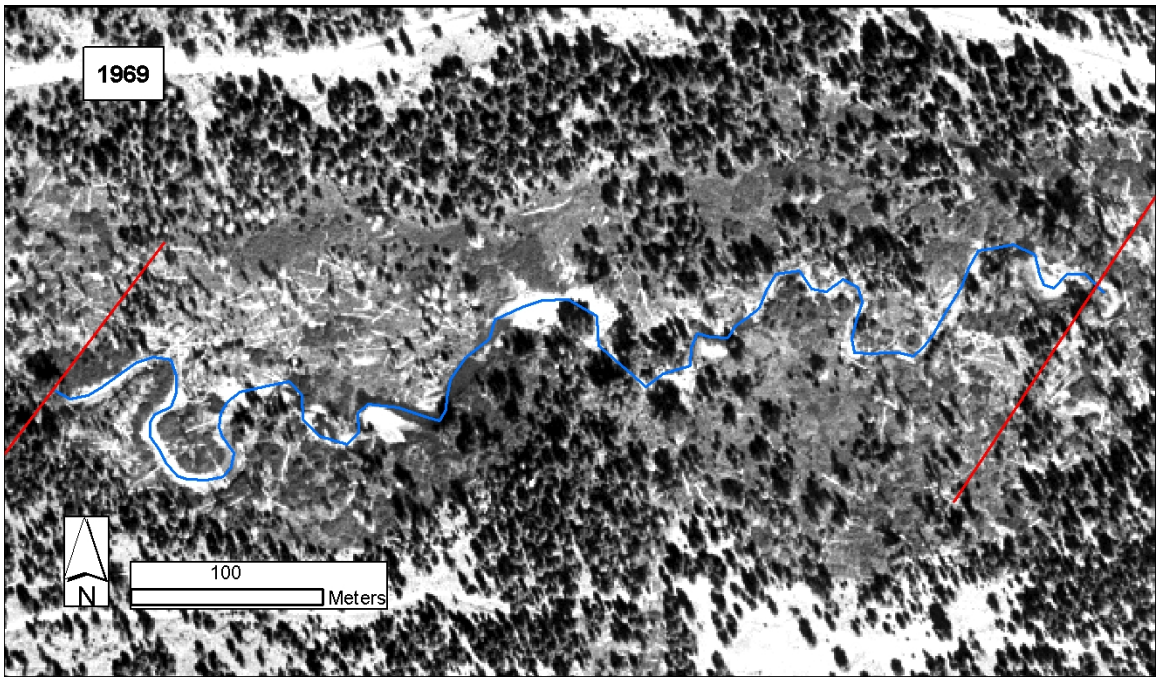

Figure 3. The 1969 aerial photo of Blackwood Creek Reach 6. The blue line is the alignment of the channel and the red lines show the extent of the Reach 6 restoration project area. Note logging on the floodplain in the western portion of the photo. Stream flow is to the east.

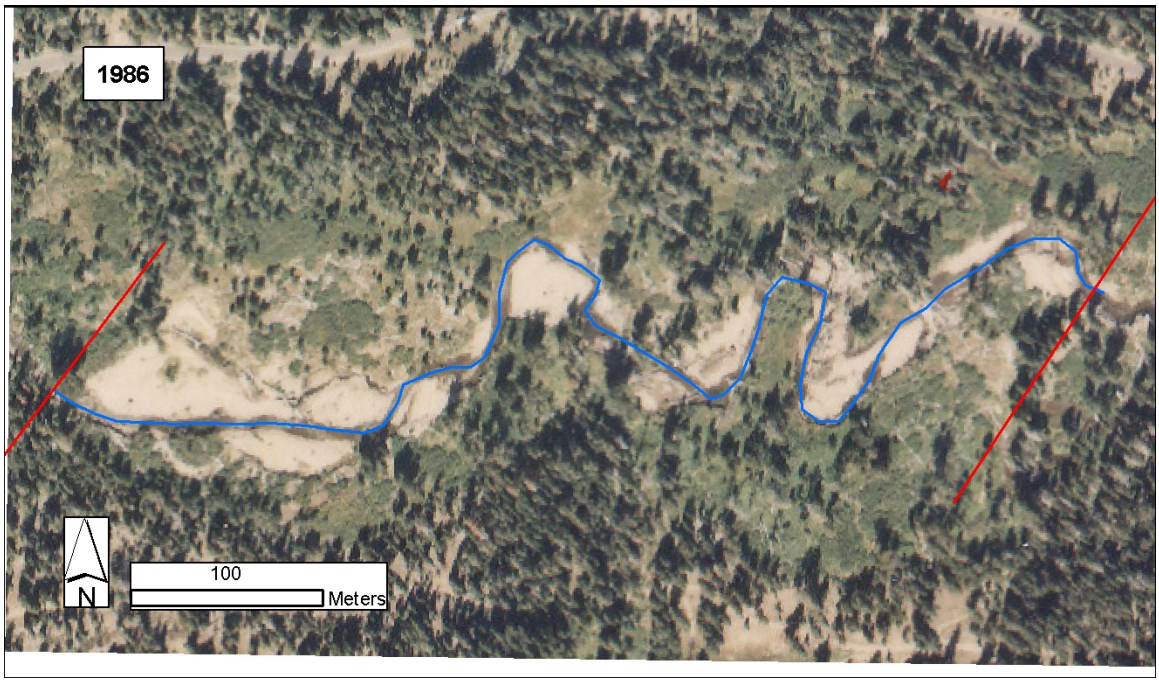

Figure 4. The 1986 aerial photo of Blackwood Creek Reach 6. The blue line is the alignment of the channel and the red lines show the extent of the Reach 6 restoration project area. Note how unvegetated washes have formed near the channel. Stream flow is to the east.

aerial photos and the 1986 photos, there were four peak flows that exceeded the five-year recurrence flow (24 m^3/s) in Reach 6. The highest peak flow in Reach 6 during this period was in 1981 at 49 m^3/s. Channel sinuosity continued to decrease in this time period, from 1.63 in 1969 to 1.53 in 1986.

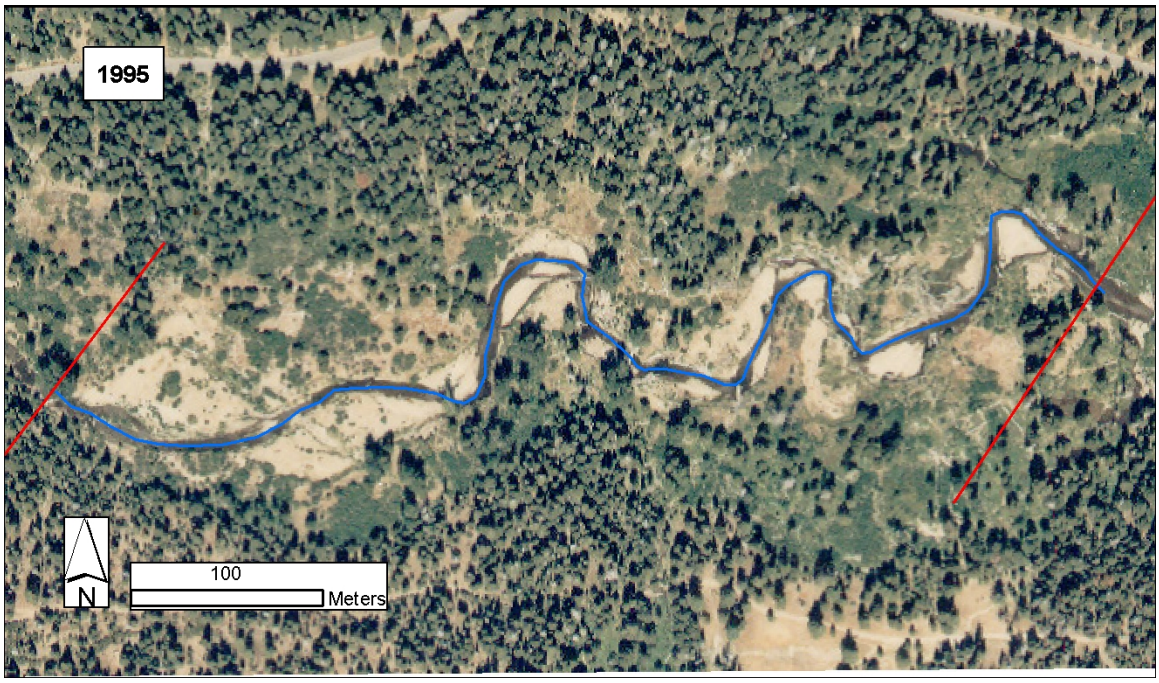

Figure 5. The 1995 aerial photo of Blackwood Creek Reach 6. The blue line is the alignment of the channel and the red lines show the extent of the Reach 6 restoration project area. Stream flow is to the east.

In the nine years between the 1986 aerial photo and the 1995 aerial photo (Figure 5), Reach 6 appeared to have changed little. During this time, there were no flows greater than the five-year recurrence, and the highest flow was 17 m^3/s in 1995. Sinuosity continued to decrease during this time from 1.53 to 1.42, due mainly to one meander being cut off.

Between the 1995 aerial photo and the 2001 aerial photo (Figure 6), the flood of record occurred in Reach 6 at 78 m^3/s with an estimated return interval of 41 years. In this six-year period, most of the vegetation that was growing on the floodplain adjacent to the channel has been replaced by open gravel washes. During this time, the channel continued to straighten and sinuosity decreased from 1.42 to 1.34.

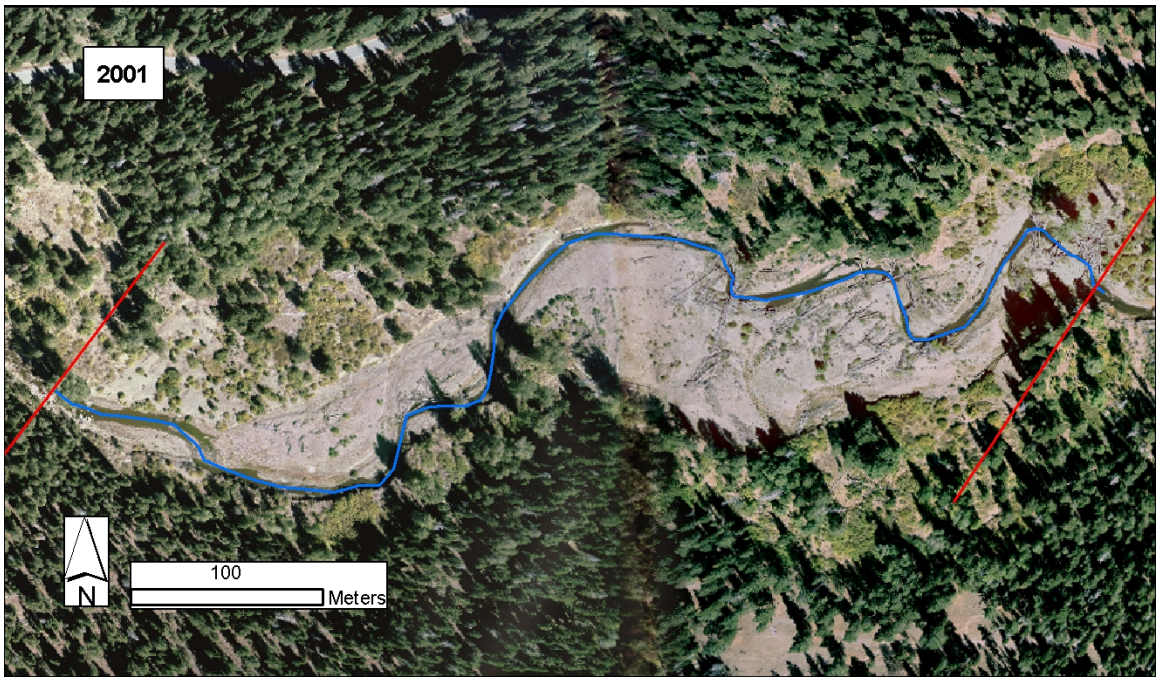

Figure 6. The 2001 aerial photo of Blackwood Creek Reach 6. The blue line is the alignment of the channel and the red lines show the extent of the Reach 6 restoration project area. Between this photo and the 1995 photo was the flood of record at78 m^3/s. Stream flow is to the east.

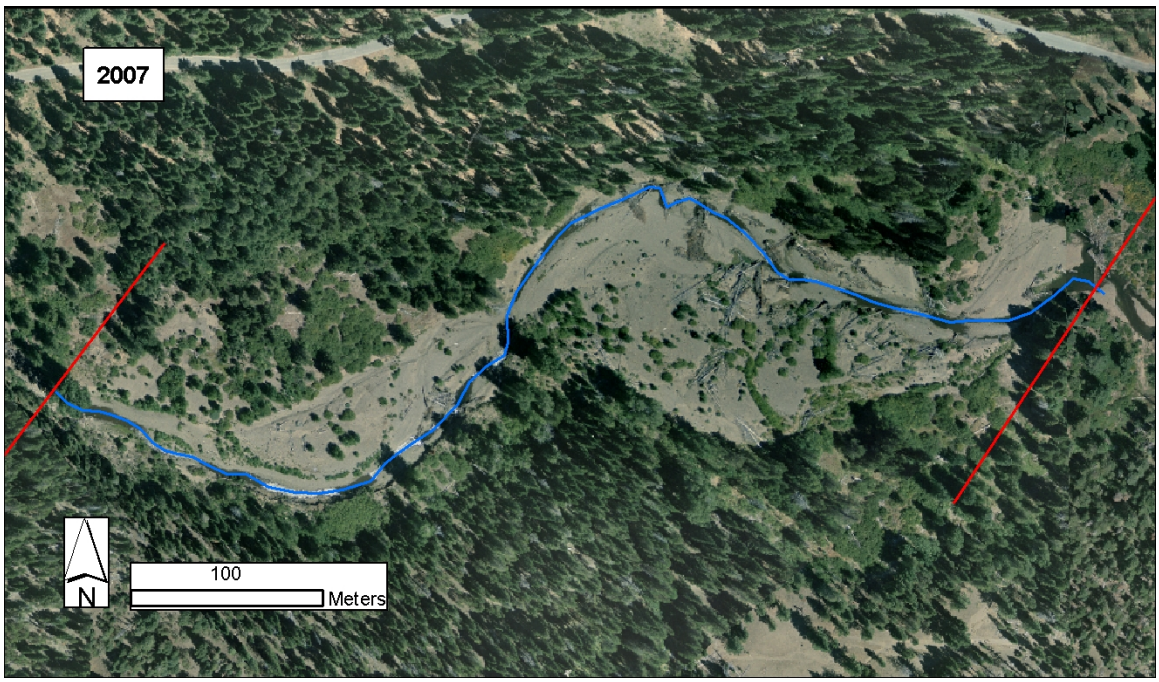

Figure 7. The 2007 aerial photo of Blackwood Creek Reach 6. The blue line is the alignment of the channel and the red lines show the extent of the Reach 6 restoration project area. By 2007, sinuosity had decreased to1.23, compared to 1.80 that was seen in 1939. Stream flow is to the east.

Tetra Tech's analysis (1999) of Reach 6 found that flows in excess of the 100-year recurrence flood would be contained within the larger capacity channel and the previous floodplain had become a terrace. In 1998, they attempted to find several historic cross sections in Reach 6. Cross section pins located in the middle of the reach could not be located due to receding channel banks due to high rates of bank erosion. They were able to locate and re-survey one cross section at the upstream end of Reach 6 in 1998. This showed that in the two years since 1996, the channel top width had increased from 12.5 m to 24 m and the cross-sectional area had increased 60% from 12.0 m^2 to 19.3 m^2.

Between the 2001 and 2007 aerial photos (Figure 7), the channel continued to straighten and decreased in sinuosity from 1.42 to 1.23. Only one flow exceeded the five-year recurrence interval during this period, and this flow was the second largest flow on record at 60 m^3/s. Combining aerial photos and repeat cross section surveys, Kiesse (2011) estimated that 12,848 m^3 of sediment was eroded out of Reach 6 between 1995 and 2001 and 1,649 m^3 was eroded out between 2001 and 2007.

Comparing this series of aerial photos of Reach 6 shows some of the changes that have occurred related to floodplain vegetation and channel sinuosity. While the cross-sectional area of the channel and floodplain cannot be ascertained from aerial photos, the changes in channel sinuosity and straightening over time can be seen between the 1939 photo and the 2007 photo. In addition to the decline in sinuosity, the decline in floodplain vegetation can be identified as the well-vegetated floodplain in the 1939 photo is replaced with unvegetated gravel washes by 2007.

1.4 Previous Restoration Work in Blackwood Canyon

The Blackwood Creek watershed has been the site of several watershed restoration projects. Most of these projects have been smaller in scale and have addressed erosion in the uplands of the watershed. The gravel mine area and the Barker Road crossing of Blackwood Creek (3.7 km upstream from Lake Tahoe) have been the primary locations for restoration work done along the stream channel (Figure 1). In 1979, the diversion channel was filled and a cement grade control structure was constructed where the creek flowed into the gravel mine site. The purpose of this structure was to prevent channel incision upstream from the lowered bed elevation of the gravel pits and allow fish passage upstream. In 2003, this cement structure was removed and a more natural functioning sequence of rock weirs was constructed that provides better fish passage. Between 1966 and 2006, this crossing consisted of a single culvert located in a causeway that extended across the floodplain. In 2005, the culvert crossing was replaced with a bridge designed to pass a 100-year recurrence flow. In conjunction with the crossing replacement, a new channel was constructed at the bridge to join the upstream and downstream channel segments.

In 2008 and 2009, the Reach 6 restoration project was implemented that is the focus of this paper. This reach was selected, because it had experienced significant straightening, incision, and bank erosion since the 1980s. The project involved constructing a new stream channel through the reach that would decrease the channel slope and increase sinuosity. Additionally, the bed elevation of the channel was raised (relative to the existing channel it replaced) and set closer to its historic channel-floodplain connection elevation. Since an excess of sediment was identified as a primary contributor to the destabilization of the reach, a design was implemented that would promote aggradation of sediment on the new channel's floodplain. An impact of

raising the channel bed elevation is that depressions were left on the floodplain. The intention was that at flood flows, the project reach would rebuild its floodplain by promoting aggradation on the floodplain throughout the reach. In addition, the project was intended to arrest the high rate of bank erosion that was continuing through the reach.

1.5 Previous Post-Project Assessment Work

Post-project appraisals take on many forms. Smith and Prestegaard (2005) performed a post-project appraisal of a stream restoration project on a reach of Deep Run in northeast Maryland. Comparing the pre-restoration condition to the as-built condition, they found that channel capacity had decreased by 30% and the sinuosity had increased slightly. One year after the project was constructed, they observed that the channel had made several adjustments in planform and cross-section area. Additionally, it was observed that several of the structures used to reduce bank erosion or maintain grade control were being compromised as channel location and capacity adjusted.

Hydraulic models can be used during post-project appraisals to predict water surface elevations and flow velocities generated by a specified flow. Klein et al. (2007) used the MIKE II hydrologic model as part of a post-project appraisal of a restoration project on the Lower Red River in north-central Idaho. This project involved constructing a new channel using the natural channel design (Rosgen, 2006) methodology. To determine if the restored reach was achieving its project objectives, the authors modeled a range of flows for the pre- and post-restoration channels to determine the predicted water surface elevation (in relation to the floodplain elevation), extent of floodplain inundation, and bankfull flow velocities. They found that the distance between the water surface elevation and the top of bank elevation was less for both

bankfull flows and low flows for post restoration conditions in 2000 (immediately after restoration work was completed) and in 2003. Comparing the modeled area inundated by water shows an increase of 150% from pre-restoration conditions. Immediately post-restoration, mean bankfull water velocity decreased significantly from pre-restoration conditions, as might be expected with a 60% increase in sinuosity.

Hydraulic models can also be used to predict the area inundated by water and shear stress generated by a specified flow. Elliott and Capesius (2009) used the HEC-RAS model to predict water surface elevation and shear stress generated in reaches of rivers in Colorado that had been altered by channel restoration activities. They compared the water surface elevations that were predicted by HEC-RAS for the 2-year, 5-year and 10-year recurrence peak flows. The model was calibrated to the observed water surface elevation during a rain-on-snow event that had occurred in the winter of 2005. The average boundary shear stress was also calculated in HEC-RAS for various cross sections. The shear stress was evaluated for the modeled flows and compared to the estimated critical shear stress. Using this method, they were able to determine whether the modeled flows produced shear stress that was greater than critical shear and were thus capable of transporting the bed material. Additionally, they were able to compare shear stresses generated at a cross section for the range of modeled flows to help understand the impact restoration work had at that location.

Thompkins and Kondolf (2007) used HEC-RAS to model flows in seven reconfigured compound channels in central California that were between two and 20 years old. They compiled cross sections and longitudinal surveys that had been surveyed after restoration work, in addition to surveying additional cross sections when there were insufficient cross sections to run the model. Manning's n values were estimated from post-project monitoring that documented the

distribution and extent of vegetation along the channel and floodplain. For each stream, the design flow for the low-flow channel and the 100-year recurrence flows were then modeled to determine water surface elevations and flow velocities. The model results were then compared to the project objectives (as stated in each project's design documentation) for conveying flood flows. They found that four of the projects were capable of passing their 100-year recurrence flow. The remaining three projects had high channel and floodplain Manning's roughness values that produced high flood stages that could flood outside of the designed floodplain of the compound channel. These projects were found to only partially achieve the stated project's objectives.

Endreny and Soulman (2011) used HEC-RAS while conducting a post-project appraisal of a stream restoration project on Batavia Kill Creek in the Catskill Mountains in New York. One of the goals of the project was to reduce bank erosion along Batavia Kill Creek. The Creek flows into a reservoir used for drinking water and was found to have above normal turbidity levels. The project was constructed using the natural channel design (Rosgen, 2006) methodology and involved constructing numerous in-channel structures designed to deflect flow away from banks and provide grade control. Using cross section and long profile survey data from 2004, two years after the project was completed, HEC-RAS modeling of the 1.3-year recurrence flow showed that flow depths in meander bend pools decreased from the as-built condition. Modeling the shear forces and hydraulic slopes for the 1.3-year return flow at cross vanes built during the project showed a hydraulic jump in the pools below the cross vanes and a shear force greater than was found in the pools that were built on meander bends. The authors attributed the decreased flow depth found in the meander bend pools to be the result of the decrease in pool shear stress, leading to aggradation.

Buchanan et al. (2010) conducted a post-project appraisal of a stream restoration project implemented on Six Mile Creek in southern New York. Here, they modeled the water surface elevation and boundary shear stress for both pre-restoration and post-restoration conditions with HEC-RAS. The shear stress for the 1.5- and 7-year recurrence flows was modeled for both pre- and post-restoration topography and then compared to a calculated critical shear stress for the channel bed D_{84}. Using this method, they were able to show that the modeled 1.5-year recurrence flow in the post-restoration channel produced an average shear stress that was lower than the pre-restoration channel and the post-restoration shear stress was less than the calculated critical shear stress. One goal of the restoration project was to promote channel stability and reduce bed and bank erosion. In reality, hydrologic modeling did not match observed conditions as cross-section surveys of the post restoration channel showed channel widening and incision throughout the restoration reach. Modeled flood flows of the restoration channel also showed that, immediately post-construction, the design channel achieved another project goal of increasing floodplain inundation.

To assess the mass balance of areas of aggradation and degradation in the project reach, Buchanan et al. (2010) also mapped out areas of fill and scour. The boundaries of the deposits were then recorded using a GPS and the data were differentially corrected. To calculate a volume for regions of fill and scour, the authors estimated the average depth of each mapped unit and multiplied by the area of the deposit. Using this method, they estimated that 24.2 m^3 of sediment deposited in the reach while 883.6 m^3 was scoured from the reach. This gave a net loss of 859 m^3 for the restoration reach.

1.6 Research Objectives

The goal of this evaluation is to document if, in the short time since implementation, restoration work in Reach 6 was successful in changing an eroding, unstable reach of channel to one that is aggrading sediment. The following describes the specific research questions for this evaluation.

1. To what degree has the channel/floodplain restoration work in Reach 6 changed the areal extent of floodplain inundation when comparing the pre-project conditions to the post-project conditions?

2. Has restoration work reduced the potential for stream channel and cut bank erosion in Reach 6 through reductions in the average boundary shear stress generated in this reach?

3. What was the approximate volume of sediment deposition that occurred on the Reach 6 floodplain during the spring runoff of 2010?

4. What are the particle size characteristics of areas of sediment deposition on the floodplain, particularly as they relate to sand and mud (< 2mm)?

Chapter 2-Methods and Data Collection

2.1 Hydraulic Modeling

The Blackwood Creek Restoration Project environmental planning documents state that two of the objectives of restoration work in Reach 6 were to "reduce fine sediment and nutrient delivery rate to Lake Tahoe through stabilization of stream channels and reconnecting channels to floodplains…" and to "restore the degraded riparian plant community through the stabilization of stream channels and reconnecting channels to floodplains." (USDA, 2008). From these stated objectives, two research questions were developed to determine if this project was successful in achieving its objectives. These questions are:

1. To what degree has the channel/floodplain restoration work in Reach 6 changed the areal extent of floodplain inundation when comparing the pre-project conditions to the post-project conditions?

2. Has restoration work reduced the potential for stream channel and cut bank erosion in Reach 6 through reductions in the average boundary shear stress generated in this reach?

To answer these questions, the project area was modeled using two software packages available from the US Army Corps of Engineers (ACE) Hydrologic Engineering Center, Hydrologic Engineering Center River Analysis Systems (HEC-RAS), and HEC Geo-RAS.

I conducted a flood frequency analysis using the log Pearson type III distribution. This analysis was carried out using the ACE Hydrologic Engineering Center's Statistical Software Package (HEC-SSP) which performs a flood frequency analysis based upon the USGS bulletin 17B, "Guidelines for Determining Flood Flow Frequency" (USGS, 1982). Annual peak flows were taken from the USGS stream gage (USGS 10336660, Blackwood Creek near Tahoe City, California), located 2 km downstream from the Reach 6 project area, which has been in continuous use since 1960. In order to develop a collection of flood flows for Reach 6, I down

scaled the flows from the USGS gage to the watershed area for Reach 6 using the guidelines of the USGS (1997).

HEC-RAS version 4.1 is a one-dimensional hydraulic modeling program that predicts water surface elevations along a stream reach and shear stress for a given discharge assuming steady flow conditions. With gradually varied flow, HEC-RAS calculates the water surface elevation at each cross section by solving the energy equation using the standard step method. This iterative process assumes that there is mass continuity between cross sections and that changes in velocity and cross-sectional area are attributed to friction loss and expansion or contraction that occurs from one cross section to the next downstream.

The core set of data required to run the model is a series of cross sections that extend across the channel and the area that might be inundated adjacent to the channel, the channel slope and length along the channel center line where each cross section lies, and a friction coefficient value (US Army, 2010). To develop this required core set of model parameters, HEC Geo-RAS was used.

HEC Geo-RAS version 4.3 is a software package that runs as an extension in Environmental Systems Research Institute's (ESRI) ArcGIS version 9.3 software. To use HEC Geo-RAS to develop the core set of model parameters, a Triangular Irregular Network (TIN) digital terrain model was needed that covers the stream channel and adjacent floodplain. The TIN for this project was generated from elevation data that consisted of 0.3-m contour lines and elevation points of the project area. A TIN is a three-dimensional surface composed of a series of interconnected triangles. For this work, the TIN was a terrain model of the channel and adjacent floodplain in Reach 6. Using HEC Geo-RAS and the three-dimensional surface of the TIN in ArcGIS, I was able to extract the information that is required to run HEC-RAS. In addition to

developing the information required to run HEC-RAS, HEC Geo-RAS has the ability to map the area inundated by water for a steady state flow modeled in HEC-RAS. To do this, the information generated from a HEC-RAS model run was loaded back into ArcGIS/HEC Geo-RAS. Using HEC Geo-RAS, a series of polygons of the inundated areas was created for a series of steady state flows.

Using this method, two TIN terrain models were created, one of the landscape as it was before restoration work, and another of the landscape as it was after restoration work. This method allowed me to compare what the modeled area inundated by water would be for identical flows by running each model with a known steady state flow. The model was run with a range of theoretical flows, and the area inundated by water was then compared between the pre-restoration conditions and the post-restoration conditions to see how the restoration project has influenced the areal extent of flood inundation.

In addition to modeling the water surface elevation, HEC-RAS has the capability to predict the average boundary shear stress generated at each cross section for a given steady flow. As HEC-RAS is a one dimensional model, calculations of shear stress do not take into account overall channel sinuosity or meander bend geometry, and therefore shear stress may be underestimated at meander bends (Richardson, 2002).

Shear stress at each cross section is calculated using equation (1):

$$\tau=\gamma R S_f \tag{1}$$

where τ is the shear stress at the cross section in N/m^2, γ is the unit weight of water in N/m^3, R is the hydraulic radius of the cross section in meters and S_f is the friction slope at the cross section (the slope of the energy grade line at the cross section). Running a series of flows through HEC-

RAS allowed me to compare the shear stress generated in Reach 6 for the pre-restoration conditions and the post-restoration conditions for each flow.

2.2 Building the HEC-RAS/HEC Geo-RAS Model

One of the primary inputs required to run the HEC-RAS 1-D model is a series of cross sections that extend across the channel and floodplain. These have traditionally been generated by field surveying a number of cross sections in the stream reach to be modeled. While cross sections measured by field surveying may be accurate, it can be time consuming to gather them.

Another method available for generating the required cross sections is to use a TIN digital terrain model in ArcGIS. Terrain models created using LIDAR or stereophotogrammetry can depict the bare earth surface of a stream's channel and floodplain, but these methods do not allow us to look into the channel below the surface of the water. To correct for this, additional surveyed information is required to depict the channel below the water surface. To account for this, Aggett and Wilson (2009) used a series of field surveyed cross sections and aerial photos to interpolate the bathymetry in a terrain model of a stream reach that was acquired with LIDAR.

On August 17, 2007, before construction was started, a series of overlapping aerial photos was acquired of Blackwood Creek that covered the Reach 6 project area. This imagery was processed by Aerial Data Inc. using stereophotogrammetry to create contour lines of the Reach 6 project area at the 0.3-m resolution. For this project, I brought the 0.3-m contour data set into ArcGIS where I created a TIN terrain model.

Using the USGS gage, 2 km downstream from Reach 6, at the mouth of Blackwood Canyon, shows the mean daily discharge was 0.04 m^3/s on the date that the 2007 aerial photos were taken. Analyzing the aerial photo shows that there was water in the pools at the time of

acquisition, but any water flowing between pools was minimal. This situation means that the contours developed using stereophotogrammetry were not able to show the bed of the channel through the water in the pools. To correct for the pool depths not accounted for in the contours, a long profile surveyed in October 2001 by Swanson Hydrology and Geomorphology was used. To account for pools in the TIN terrain model, pool depth contour lines were interpolated in ArcGIS at similar depths to what was measured in the long profile. The TIN was then created from the 0.3-m contour lines that accounted for pool depths.

On November 3, 2010, after the restoration project was completed, another series of aerial photos was acquired and processed by Aerial Data Inc. They used stereophotogrammetry to create 0.3-m contour lines of Reach 6. On this date, the USGS gage at the mouth of Blackwood Canyon had a mean discharge of 0.22 m^3/s. Analyzing the aerial photo showed that there was water in the pools in Reach 6. As in the 2007 TIN Terrain model, the pools were not included in the derived contours as the stereophotogrammetry technique will not penetrate below the water surface. To correct for the pool depths not accounted for in the contours, a series of total station points collected in fall 2009 by Water Ways Consultants was used. I brought these points of known channel bed elevation into ArcGIS, and interpolated contour lines around them. Using these additional contour lines, I was able to create pools in the TIN that were similar to the surveyed pool depths. With the two TIN terrain models built and HEC Geo-RAS, I was able to extract the information that is needed to run HEC-RAS. Because the TIN terrain model is a three-dimensional surface, two-dimensional data (channel center line, channel banks, distance between cross sections along the channel center line) and three-dimensional (channel cross sections, channel slope) data can be extracted from the TIN (US Army, 2009).

Discharge m^3/s	Manning's n
5.18	0.0465
5.32	0.0325
2.01	0.0361
1.95	0.0664

Table 3. Table 3 shows the discharge measurements taken in July 2011 and the Manning's n that was calculated for that discharge.

With the terrain models built for the pre-construction and post-construction conditions, a Manning's n value was selected. To select an n value for the channel, the slope of the channel was surveyed and a series of flow measurements were taken in July 2011 (Table 3). Using these measurements and the equation (2) for Manning's n:

$$V=(R^{2/3}S^{1/2})/n \tag{2}$$

where V is the average water velocity in m^3/s, R is the hydraulic radius of the channel with flow in meters, S is the channel slope, and n is Manning's n (Chow, 1959). Multiplying both sides of equation (2) by n, and dividing by V, with V equal to the discharge (Q) divided by the area (A), yields equation (3):

$$n=(R^{2/3}S^{1/2}A)/Q \tag{3}$$

Solving for n with equation (3), using the cross section measurements and Q from the discharges measured in Reach 6, gives an n value for each discharge measurement. Taking the average of the calculated n values, I got an n of 0.045.

In Ven Te Chow's Open Channel Hydraulics (Chow, 1959) the author provides a table of Manning's n values for various natural stream channels and floodplains. Chow's proposed range of values for "Mountain streams, no vegetation in channel, banks usually steep, trees and brush along banks submerged at high stages" with a "Bottom: gravel, cobbles, and few boulders" is a

minimum of 0.03, a maximum of 0.05, and a normal value of 0.04. Comparing the field calculated channel n value of 0.045 to Chow's proposed values shows that this value is within his proposed range, but near the high end. As floodplain roughness is generally greater than channel roughness, the calculated channel n value was doubled to give us a floodplain n value of 0.09.

On the evening of June 6, 2010, I visited Reach 6 and took a series of photos between 17:30 and 19:00. The peak flow for the 2010 water year was 13.1 m^3/s and occurred on this date at 18:15, according to the USGS gage at the mouth of Blackwood Canyon. The peak flow in Reach 6 was estimated by scaling the peak flow at the gage to the watershed area of the lower end of Reach 6 which gave a flow of 12.3 m^3/s. In November 2011, these photos were used to determine the water surface elevation at several locations along the length of the constructed channel in Reach 6. The elevation of these locations was mapped using GPS, surveyed, and tied into the same datum used to build the HEC Geo-RAS terrain model. The 2010 HEC RAS model was then calibrated by adjusting the Manning's n value until the modeled water surface elevations were similar to the surveyed elevations for a flow of 12.3 m^3/s. This calibration lowered the original estimates of n to 0.04 for the channel and 0.08 for the floodplain. Table 4 compares the surveyed elevations and modeled elevations for the series of points used in the model calibration to the 12.3 m^3/s discharge.

In summer 2010, after the spring snowmelt peak, field mapping was conducted to map the extent of the project that was inundated by water. Mapping was done by using the series of photos taken during the spring 2010 peak flow, then looking for high water stage indicators such as areas of organics deposited on the edges of the floodplain and floodplain surfaces that were re-organized or sorted by the passing of the high water stage. Since the restoration work was

Distance Upstream from Bottom or Reach 6 Project Boundary (m)	Surveyed Water Surface Elevation (m)	HEC-RAS Modeled Water Surface Elevation (m)	Elevation Difference (Surveyed - Modeled) Elevation (m)
75	1,922.40	1922.35	0.05
245	1,923.49	1923.54	-0.05
710	1,926.06	1926.06	0.00
765	1,926.36	1926.39	-0.03
770	1,926.35	1926.38	-0.03
775	1,926.35	1926.39	-0.04
785	1,926.38	1926.37	0.01
983	1,927.70	1927.69	0.01
988	1,927.71	1927.69	0.02

Table 4. This table compares the water surface elevation with the modeled water surface elevation once the HEC-RAS model was calibrated to a discharge of 12.3 m^3/s. Distance upstream is the distance up the channel from the downstream Reach 6 project boundary. The elevation difference is the surveyed elevation minus the modeled elevation.

completed in fall 2009, and this event was the first flow to inundate the floodplain, any indicators of high water stage in the project area were assumed to be from the spring 2010 peak flow. The location of field indicators of high water stage were recorded with a Trimble GeoXT GPS, and the data were differentially corrected to remove any atmospheric disturbances at the time of acquisition. These data were then brought into ArcGIS, and a polygon of the area inundated by water was created from these field indicators. The mapped extent of flooding is very similar to the modeled area inundated by water for the same discharge. While the modeled flood did not capture all of the islands sticking up within the area of flooding, the outer limits of the mapped flood and the modeled flood were quite similar.

HEC-RAS was run with the 2007 and 2010 models using the flows shown in Table 5. For each flow that was modeled, HEC-RAS calculated the water surface at each cross section and the shear stress that was generated at that cross section. After the HEC-RAS model was run, the model output was brought back into HEC Geo-RAS. Using HEC Geo-RAS, I was able to convert the water surface elevation found at each cross section into a series of polygons of the

Event	Flow (m^3/s)
1.5-year peak	7.4
2-year peak	10.7
2.3-year peak (spring 2010 peak)	12.3
3-year peak	16.0
4-year peak	20
5-year peak	23
10-year peak	37
15-year peak	47
20-year peak	55

Table 5. This table shows instantaneous peak flows at Reach 6 used to model the area inundated by water and shear stress. Flows were acquired from the USGS gage #10336660, Blackwood Creek Near Tahoe City California located at the mouth of Blackwood Canyon (USGS, 2011) and scaled down to the watershed for Reach 6.

area inundated by water. All the polygons were then trimmed to the upstream and downstream extents of the Reach 6 restoration project area. The area of each polygon was then calculated, and the 2007 and 2010 areas were compared for each flow.

Once the models were run in HEC-RAS, I also compared the average boundary shear stress generated by each flow. HEC-RAS calculates the shear stress at each cross section for a given flow, and gives a value for each cross section. Cross sections extended across the channel and floodplain. The number and location of cross sections is different in the pre-restoration and post-restoration models. In order to compare the difference in shear stress between the pre-restoration conditions and the post-restoration conditions, the mean cross section shear stress was calculated for each flow. Using these values, I compared how the shear stress had changed from pre-restoration conditions to post-restoration conditions for the same flow.

2.3 Sediment Deposition/Scour Mapping and Sampling

The Blackwood Creek Phase III, Stream and Floodplain Restoration Project Environmental Assessment states that one of the objectives of restoration work in Reach 6 was to

"Reduce fine sediment and nutrient delivery rate to Lake Tahoe through stabilization of stream channels and reconnecting channels to floodplains…" (USDA, 2008). From this objective, two research questions were developed that will be used to help us determine if this project was successful in achieving these objectives. These questions are:

1. What was the approximate volume of sediment deposition that occurred on the Reach 6 floodplain during the spring runoff of 2010?
2. What are the particle size characteristics of areas of sediment deposition on the floodplain, particularly as they relate to sand and mud (< 2mm)?

During the spring snowmelt of 2010, Blackwood Creek Reach 6 had a peak flow of 12.3 m^3/s (a 2.3-year recurrence peak flow). This was the highest peak flow to occur since the Reach 6 restoration project was completed in October 2009. After flows dropped in summer 2010, areas of scour and new areas of deposition were observed within the project area. In order to document the changes that occurred, I mapped the areal extent and average depth of areas of scour and deposition.

The areal extent of areas of deposition and scour was mapped in two ways. The boundaries of some deposit/scour areas were recorded using a Trimble GeoXT GPS. Once collected, these data were differentially corrected to remove any atmospheric disturbances at the time of acquisition and the data were brought into ArcGIS. Another technique used in mapping was to use a tape measure to measure the extent of the area of deposit/scour and hand draw the shape onto a base map of the project area. This hand-drawn map was then scanned and georeferenced in ArcGIS, and polygons were digitized around the hand-drawn areas. These digitized areas were then checked against field notes to determine if the area of the polygon digitized was similar in surface area to the surface area of the deposit/scour area measured in the field. This method of mapping polygons was used when satellite reception was poor or when

polygons were either small or long and narrow. In the latter case, measuring the polygon in the field was thought to be a better method of mapping as the opposing edges of the polygons were so close that they might be within the resolution of the GPS.

In many locations, adjacent deposition polygons share a common boundary. In these cases, the polygons were mapped as being distinct from one another by some distinguishing characteristic such as the estimated median surface grain size (D50) and/or the estimated average depth of the deposit at the time that the deposit was mapped.

Areas that were identified as being reorganized during the high flow, but were not predominantly an area of deposition or scour, were also mapped using these same methods. As these polygons contained a mixture of both deposition and scour, these polygons were labeled as mixed polygons.

In order to calculate volumes for deposition and scour in the project, I needed to have a thickness to assign to each polygon of deposition/scour. Average thicknesses for deposition polygons were measured using two methods. Deposits that that were less coarse were probed for depth using a V-Star rod. This is a stainless steel rod with depth increments on the side. The rod was pressed vertically into the deposit until coarser, more resistant material under the deposit was encountered. In deposits of coarser material, shovels were used to dig through the deposit to identify the thickness of the deposit. In most locations, a boundary could be clearly identified between the underlying surface that was constructed during the restoration work and the overlying deposits which tended to be better sorted. The number of locations that thickness was measured varied for each polygon. Measurement locations were taken near the edges and in the middle of the mapped deposits. In some deposits, especially the fine sediment deposits, there were areas where the thickness of the deposit was much greater than the rest of the mapped

polygon boundary. This was frequently found on the downstream side of logs or rocks on the floodplain that created an area of low velocity water where fines would aggrade. These areas of thicker than normal deposits were considered outliers and were not used to determine the average deposit thickness.

A random approach was used to determine the number of measurements taken. No standard number of measurements was used. The number of measurements taken was determined in the field based on my professional judgment regarding how many measurements were needed to determine an average thickness for that particular polygon. The number of measurements was based upon the size of the polygon and the variability of the measurements as they were taken. Individual measurements were not recorded; rather, measurements were taken until a reasonable estimate of the average thickness could be determined. Larger deposits were sampled in more locations than smaller deposits, and the thicker deposits were sampled in more locations than thinner deposits. Deposits that were found to have greater variability in the measured depth were sampled more extensively than were deposits that had more uniform thickness measurements. The smallest polygons were sampled in at least four locations, and the largest polygons were sampled in more than 20 locations.

For estimates of areas of scour, assumptions had to be made as to the shape of the landscape before it was removed. Many of the areas of scour were associated with side channels across the floodplain and areas of bank scour adjacent to the main channel. At the locations of new side channels across the floodplain, it was assumed that the channel formed in material that was previously at the same elevation as the surrounding material. These new side channels were mapped (for surface area and depth) as an area of scour. For areas of bank erosion, it was assumed that the banks in the area scoured were similar in shape to the banks immediately

upstream and downstream that showed no signs of scour. In addition, photos taken immediately post-project were referenced to assist in determining the extent of deposition and scour.

In order to characterize the grain size distribution of areas of deposition in the project, samples were gathered within the mapped areas of deposition. To do this, the deposits were first categorized by their surface grain size. Deposits were classified into one of three classes based upon a visual estimate of the D50 of the surface of the deposit. Fine deposits, i.e. sand and mud, had a surface D50 of less than 2mm, medium deposits had a surface D50 of 2mm to 16mm, i.e. very fine, fine and medium gravels and coarse deposits had a D50 greater than 16mm, i.e. coarse gravel, very coarse gravel and cobbles. ArcGIS was then used to select the polygons with the largest surface area within each of the three size classes. Nine samples were gathered in the fine size class, nine samples were taken in the medium size class, and ten samples were gathered in the coarse size class.

In an effort to not bias the sampling location, the following method was used to select the location on the deposit to sample. First, the long axis of the mapped deposit was measured and a number from 0 to 100 was drawn from a bag. This number was then used to select the percent along the tape measure where I would next place the tape measure. At the selected location, the tape measure was stretched perpendicular to the first alignment. Once again, a number was drawn and used to determine the percent along the second tape measure alignment where the sample would be taken. Using this method, 28 bulk samples were gathered in one-gallon Zip-Lock bags. At each sampling location the top layer of the deposit was removed before the sample was collected to try to remove any armoring that may be present. This layer removed was equal to two times the estimated D50 of the surface deposit.

Bunte and Abt (2001) propose that the minimum bulk sample size mass required to obtain a representative sample can frequently be approximated by taking 20 to 100 times the mass of the D_{max} (the single largest particle in the sample). Table 6 compares the dry sample mass to the D_{max} mass of the medium and coarse samples. Of the 19 samples, two did not achieve the minimum of 20 times the total sample mass, and all the medium samples fell within the 20 to 100 times minimum range they proposed. As the main goal of this project was to determine the grain size characteristics of the fine size class, all samples collected were used, including the two whose sample mass was less than 20 times D_{max}. Field sieving was not used as samples needed to be wet sieved in order to remove all the finer material from the coarser material in the sample, and therefore needed to be processed in a laboratory.

While it is impossible to precisely characterize the areas of scour in the project area, an effort was made to try to determine what the grain-size distribution may have been. With the exception of the imported boulders (imported material was predominantly greater than 30 cm in diameter), all materials used in the construction of the project in Reach 6 came from the site. This means the mixture of mud, sand, gravel, and cobbles present within the Reach 6 channel and floodplain before restoration is also present within the project area after restoration. To try to characterize what the grain-size distribution may have been for the areas of scour, three locations were chosen to sample. All three locations were in areas that did not appear to have been submerged by the spring 2010 high water stage and were immediately adjacent to areas of bank scour that were mapped along the main channel. Material from these three locations was collected and combined together for processing as one sample.

The bulk sediment samples collected in Reach 6 were then processed for grain size analysis by the Desert Research Institute (DRI) in Reno, NV. First, the samples were oven dried

Sample ID #	Size Class	Total Sediment Dry Mass (g)	D_{max} (g)	Total Sediment Dry Mass (g)/D_{max}(g)
C11-802	Coarse	3,043	290	10.5
C11-803	Coarse	3,691	78	47.3
C11-804	Coarse	5,264	189	27.9
C11-805	Coarse	4,805	222	21.6
C11-806	Coarse	5,361	756	7.1
C11-807	Coarse	4,067	120	33.9
C11-808	Coarse	4,468	152	29.4
C11-809	Coarse	3,565	126	28.3
C11-810	Coarse	4,099	198	20.7
C11-811	Coarse	2,971	78	38.1
C11-812	Med	3,917	162	24.2
C11-813	Med	3,887	75	51.8
C11-814	Med	3,310	25	132.4
C11-815	Med	3,512	152	23.1
C11-816	Med	2,945	72	40.9
C11-817	Med	3,524	62	56.8
C11-818	Med	2,399	18	133.3
C11-819	Med	3,427	97	35.3
C11-820	Med	1,114	20	55.7

Table 6. This table compares the dry bulk sample mass to the mass of the largest single particle in the sample for bulk samples.

overnight. If organic matter was present, it was burned off. The samples were then dry sieved with a 2-mm sieve to separate the gravel and cobbles from the finer fraction. The sand and mud was then wet sieved with a 62.5-um sieve to separate the sand from the mud, and each sample was then dried and weighed. From the mud (<62.5um) portion of the sample, a subsample volume was taken to run through a Micromeritics Saturn DigiSizer 5200 laser particle size analyzer. Using this method, I estimated the percent of silt and clay from the analyzed mud subsample by volume. I then used these percents to determine the percent silt and clay for the entire <62.5 um portion of the sample, with the assumption that the subsample was representative of the <62.5 um portion.

I combined the grain-size distribution data for sand, gravel and cobble (percent by weight) with size distribution data for the silt and clay (percent by volume). To combine these I assumed that the density of the silts and clays is similar to the other material in the sample. This is a common assumption made by researchers and should be a reasonable assumption as the common density range proposed for clays is 2.6 - 2.8 g/cm^3 (US Department of Energy, 2011). This density range is close to the density range proposed for andesitic rocks (2.65 g/cm^3) (Edumine, 2011) that are prevalent in the watershed (California Geologic Survey, 2005). With this assumption, I combined the <62.5 um grain-size distribution data (a distribution by volume) with the grain-size distribution of the gravel+ and sand (done by weight). Combining these gave me a grain-size distribution of each sample by weight.

In order to develop a weight to volume ratio for the sample, the volume of each sample was measured. Using the grain-size distribution data by weight (in grams) and the volume of the sample (in liters), I was able to determine the density in g/L of each particle size class for each sample. Samples were then grouped according to their surface D50 used in the sediment deposit/scour mapping, and the average density (g/L) of each particle size in the size distribution was calculated. I then took the volume of each sediment feature mapped and multiplied by the density for a given particle-size class to determine the weight of that volume within the sediment feature.

Chapter 3-Results and Discussion

3.1 Hydraulic Modeling

The area inundated by water at Reach 6 has increased at all flood flows that were modeled for this project (Table 7). The lowest peak flow modeled was the 1.5-year peak flow at 7.4 m^3/s. This discharge produced the greatest percentage increase in water inundation between pre-restoration conditions and post-restoration conditions with a 106% increase (area of flooding increased from 14,200 m^2 to 29,300 m^2). The largest peak flow modeled was the 20-year peak flow at 55 m^3/s, and this saw an increase in flooded area of 27% from 38,200 m^2 to 48,400 m^2. Looking at Table 7 shows a trend where, for the range of flows modeled, the lowest magnitude

Event	Flow (m^3/s)	Pre-Restoration Flooded Area (m^2)	Post-Restoration Flooded Area (m^2)	Increase or Decrease in Flooded Area after Restoration	Change in Flooded Area (m^2) from Pre-Restoration to Post-Restoration	Percent Change
1.5-year peak	7.4	14,200	29,300	Increase	15,100	106
2-year peak	10.7	16,100	32,300	Increase	16,300	101
2.3-year peak (spring 2010 peak)	12.3	16,800	33,100	Increase	16,400	97
3-year peak	16	18,800	34,700	Increase	15,900	85
4-year peak	20	21,000	36,400	Increase	15,400	74
5-year peak	23	25,400	37,700	Increase	12,300	48
10-year peak	37	31,400	43,000	Increase	11,600	37
15-year peak	47	35,600	46,300	Increase	10,800	30
20-year peak	55	38,200	48,400	Increase	10,200	27

Table 7. This table compares the modeled flooded area between the 2007 pre-restoration conditions and the 2010 post-restoration conditions for a range of flows.

peak flows have the greatest percentage increase in the change between pre-restoration flooded area extent and post-restoration flooded area extent, and the largest magnitude peak flows have the smallest increase. Figure 8 shows the flood frequency graph of the scaled flows for Reach 6.

The average cross section shear stress has decreased for all flood peak flows that were modeled for this project (Table 8). The 1.5-year recurrence peak flow is 7.4 m^3/s and saw a

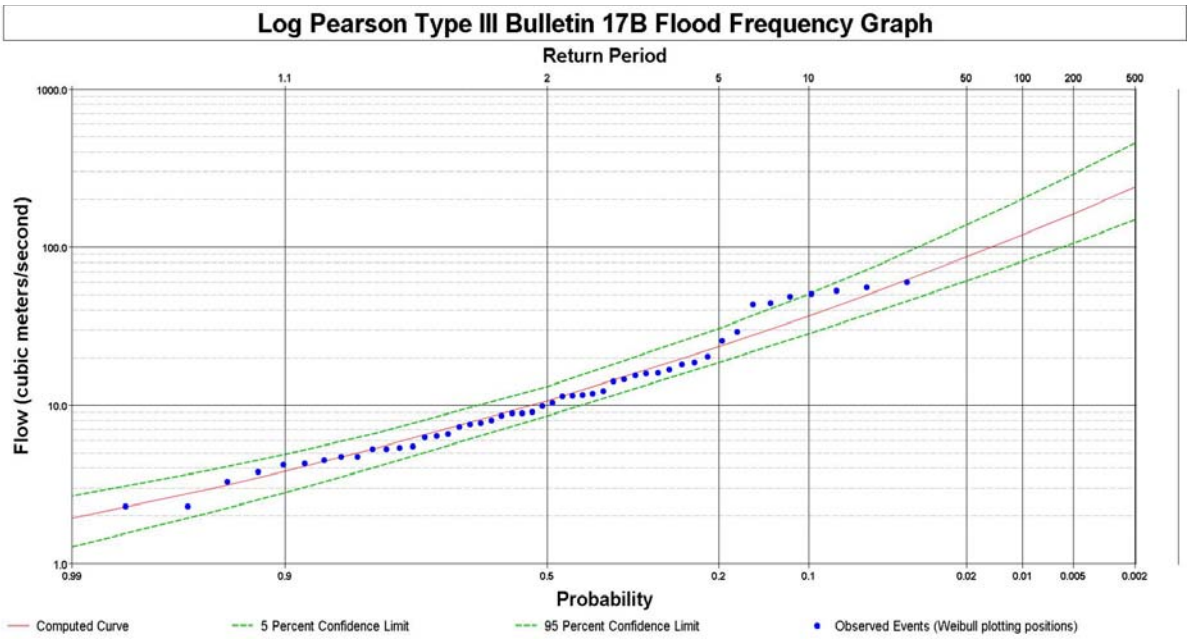

Figure 8. Log Pearson type III flood frequency analysis for the downstream end of Blackwood Creek Reach 6. Instantaneous peak flows were taken from the USGS gage #10336660, Blackwood Creek Near Tahoe City California located at the mouth of Blackwood Canyon (USGS, 2011) and scaled down to the watershed for Reach 6.

		Average Cross-Sectional Shear Stress			
Event	**Flow m^3/s**	**Pre-Restoration (N/m^2)**	**Post-Restoration (N/m^2)**	**Increase or Decrease in Shear Stress after Restoration?**	**Percent change**
1.5-year peak	7.4	37.5	23	Decrease	-39%
2-year peak	10.7	43.2	26.3	Decrease	-39%
2.3-year peak (peak flow of spring 2010)	12.3	45.7	28	Decrease	-39%
3-year peak	16	50.4	29.9	Decrease	-41%
4-year peak	20	52.7	29.5	Decrease	-44%
5-year peak	23	54	31.4	Decrease	-42%
10-year peak	37	58.2	33	Decrease	-43%
15-year peak	47	64.8	36.2	Decrease	-44%
20-year peak	55	69.4	36.3	Decrease	-48%

Table 8. This table shows the average cross-sectional shear stress that was modeled in HEC-RAS for pre-restoration conditions and post-restoration conditions for a range of flows.

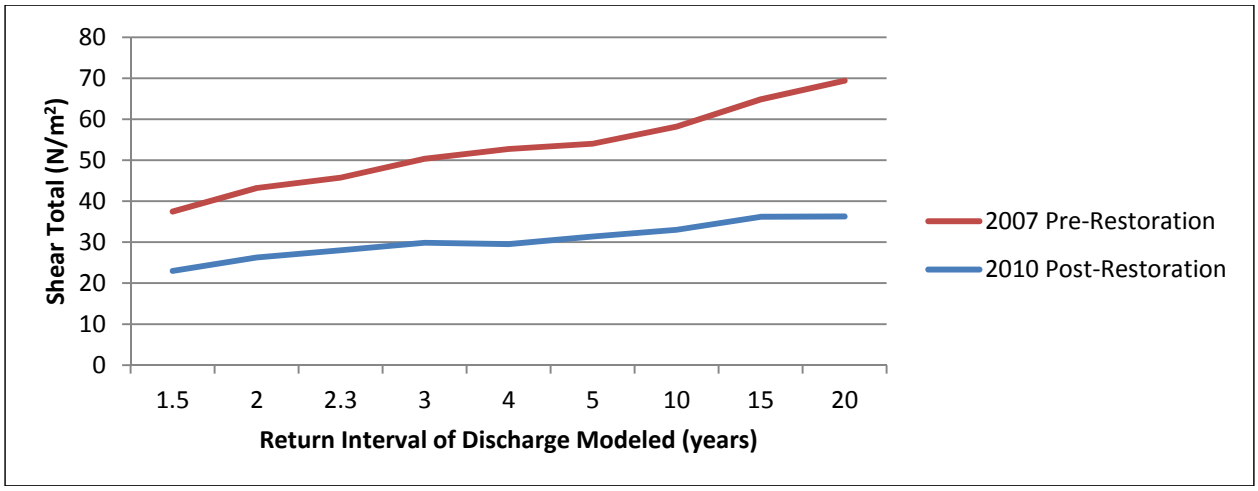

Figure 9. This graph shows the average cross section shear stress of the channel and floodplain that was modeled in HEC-RAS for pre-restoration conditions and post-restoration conditions for a range of flows.

decrease in average cross-sectional shear stress of 39%. The greatest difference was for the 20-year recurrence peak flow that had a decrease in average cross-sectional shear stress between pre-restoration and post-restoration conditions of 48%. Figure 9 shows that the modeled values for average cross-sectional shear stress increased with discharge for both the pre-restoration conditions and post-restoration conditions. This figure also shows that as discharge increased, the difference between pre-restoration and post-restoration conditions also increased as the pre-restoration average cross-sectional shear stress increased more rapidly. This means that for the range of modeled values, the difference in average cross-sectional shear stress is less for the lower recurrence peak flows and greater for the less common, longer recurrence peak flow.

3.2 Sediment Deposition/Scour Mapping and Sampling

Comparing the area of the mapped regions of deposition, scour, and mixed areas (areas showing a mixture of deposition and scour), shows that there are 11,560 m^2 of deposition, 591 m^2 of scour and 729 m^2 of mixed (Table 9). This change means that there was nearly 20 times more deposition area than scour area. Comparing the calculated volumes shows that there was

1,129 m^3 of deposition and 142 m^3 of scour in Reach 6. This means that there was roughly seven times more deposition volume than scour volume. While the area of scour mapped and volume of scour calculated were both less than for deposition, the difference between them is less once the volume of the deposits is calculated. This was because the areas of scour tended have a greater average depth, as many of the mapped areas of scour were where bank erosion occurred. The greatest depth assigned to any area of deposition or scour was 1.5 m where bank erosion occurred. While there is, of course, some uncertainty involved with the mapping of areas of sediment deposition and scour and in estimating the thickness of such areas, there seems to be a clear trend in this data of a greater volume of deposition than volume of scour.

	Surface Area (m^2)	**Volume (m^3)**
Deposit	11,560	1,129
Scour	591	142
Mix	729	na

Table 9. This table shows the area and volume of areas of deposition, scour and mixed areas (areas showing a mixture of deposition and scour) that were mapped in the summer of 2010 in Reach 6.

Combining the sediment deposition/scour volumes with the sediment sampling data shows some of the characteristics of the deposited material and the scoured material. Looking at Table 10 shows that there were 623 Mg of gravel and coarser (>2mm), 776 Mg of sand, 114 Mg of silt and 28 Mg of clay deposited in Reach 6, and there were 188 Mg of gravel and coarser

	Gravel+	**Sand**	**Silt**	**Clay**	**Total**
Total Weight in Deposit	623 Mg	776 Mg	114 Mg	28 Mg	1,541 Mg
Total Weight in Scour	188 Mg	83 Mg	7 Mg	3 Mg	281 Mg
More Deposition or Scour?	Deposition	Deposition	Deposition	Deposition	Deposition
Difference	435 Mg	693 Mg	107 Mg	25 Mg	1,260 Mg

Table 10. This table shows weight in megagrams of the gravel and coarser, sand, silt and clay in the areas of deposit and scour. Also shown is whether there was more deposition or scour for each size class and what the difference was between the two values.

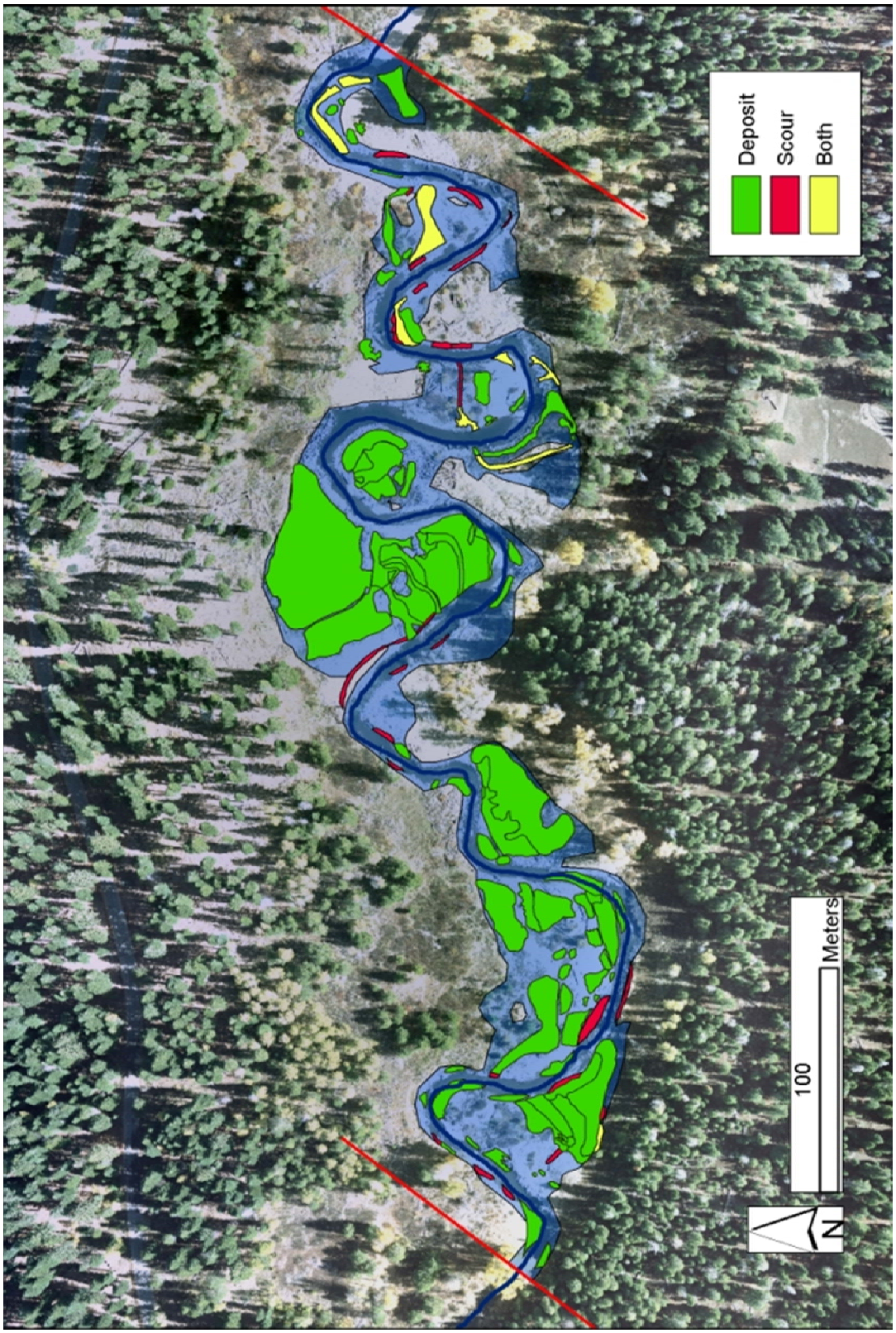

Figure 10. Map showing the modeled area inundated with water by the HEC-RAS/HEC Geo-RAS modeled 2.3-year, 12.3 m^3/s flow and the areas of deposition, scour and areas that had both deposition and scour that were mapped in the summer of 2010.

(>2mm), 83 Mg of sand, 7 Mg of silt and 3 Mg of clay scoured. Of the four size classes used in this study, sand was the class that had the greatest amount of deposition with 776 Mg. As was stated previously, there is greater uncertainty with the grain-size distribution information for the scoured areas because this estimate is for material that is no longer there.

Comparing the weight of each size class of deposition and scour shows that all size classes had more deposition than scour. The greatest difference between deposition and scour was for the sand size class where there was a difference of 693 Mg between deposition and scour. Figure 11 displays the relative weights of scour and deposition by size class.

Looking at the locations of deposition and scour (Figure 10) shows several patterns. The coarse deposits that were mapped tended to be adjacent to the channel. This pattern is expected as flows over the floodplain would be slower than along the channel and would therefore be less competent to transport larger particles. The majority of fine deposits were mapped in depressions on the floodplain that were left during construction of the restoration project and down-valley from the roughness structures. Here, far from the thalweg, where flow velocities would be low

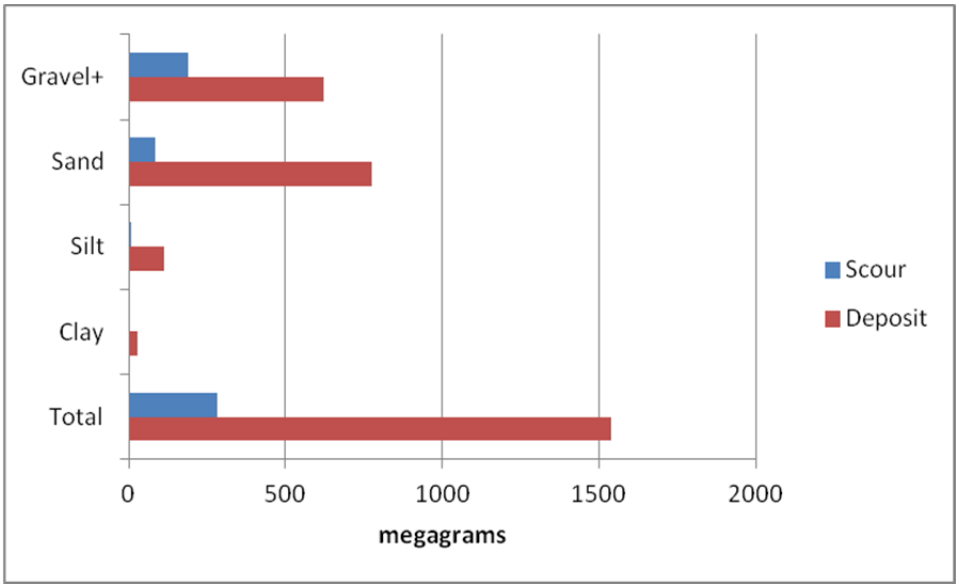

Figure 11. The weight in megagrams of the deposition and scour for each size class used in this study as well as the total weight of deposition and scour.